

Supporting Information

Why the Reactive Oxygen Species of the Fenton Reaction Switches from Oxoiron(IV) Species to Hydroxyl Radical in Phosphate Buffer Solutions? A Computational Rationale

Hsing-Yin Chen

Department of Medicinal and Applied Chemistry, Kaohsiung Medical University, Kaohsiung 80708, Taiwan

E-mail: hychen@kmu.edu.tw

Table of Contents

- Page S2. Gas-phase electronic energy change of $[\text{Fe}^{\text{II}}\text{H}_2\text{O}]^{2+} + \text{H}_2\text{PO}_4^- \rightarrow [\text{Fe}^{\text{II}}\text{H}_2\text{PO}_4]^+ + \text{H}_2\text{O}$.
- Page S2. Hydration energies of H_2O and H_2PO_4^- .
- Page S3. Free energy change of successive H_2O exchange by H_2PO_4^- for $[\text{Fe}^{\text{II}}(\text{H}_2\text{O})_6]^{2+}$.
- Page S4. Average bond distances and standard deviations for ADMP dynamics simulation of $[\text{Fe}^{\text{II}}(\text{H}_2\text{PO}_4)_5(\text{H}_2\text{O})]^{3-}$.
- Page S5. Calculated $\langle S^2 \rangle$ values.
- Page S6–S7. ADMP dynamics simulations of $[\text{Fe}^{\text{II}}(\text{H}_2\text{PO}_4)_5(\text{H}_2\text{O})]^{3-}$.

Table S1. Gas-phase electronic energy change (kcal/mol) of $[\text{Fe}^{\text{II}}\text{H}_2\text{O}]^{2+} + \text{H}_2\text{PO}_4^- \rightarrow [\text{Fe}^{\text{II}}\text{H}_2\text{PO}_4]^+ + \text{H}_2\text{O}$.

method	ΔE
B3LYP-D3/6-31+G(d)	-301.7
PBE0-D3/6-31+G(d)	-301.9
M06-D3/6-31+G(d)	-303.5
PW6B95-D3/6-31+G(d)	-296.9
PW6B95-D3/Def2-TZVP	-300.3
PW6B95-D3/Def2-QZVP	-300.0
BD(T)/Def2-TZVPP	-293.4

Table S2. Hydration energies (kcal/mol) of H_2O and H_2PO_4^- . Signed errors are given in parentheses.^a

method	H_2O	H_2PO_4^-
SMD/PW6B95-D3/6-31+G(d) ^d	-9.3 (-3.0)	-76.9 (-8.9)
IEF-PCM/PW6B95-D3/6-31+G(d) ^d	-5.4 (0.9)	-67.1 (0.9)
CPCM/PW6B95-D3/6-31+G(d) ^d	-5.5 (0.8)	-67.2 (0.8)
Expt.	-6.3	-68

^a Theoretical hydration energies were evaluated by the difference between solution-phase electronic energy and gas-phase electronic energy at solution-phase optimized geometry.

Table S3. Free energy change (kcal/mol) of successive H₂O exchange by H₂PO₄⁻ for [Fe^{II}(H₂O)₆]²⁺.^a

n	CPCM/PBE0/6-31+G(d)	SMD/PBE0/6-31+G(d)	CPCM/M06/6-31+G(d)	CPCM/PW6B95/6-31+G(d)	CPCM/PBE0/Def2-TZVP ^b	CPCM/PBE0/Def2-QZVP ^b
1	-16.5	-13.7	-15.5	-17.4	-18.1	-16.9
2	-14.8	-12.9	-14.6	-15.2	-16.3	-15.4
3	-13.1	-13.4	-11.5	-10.8	-16.4	-14.2
4	-11.8	-13.3	-11.0	-13.6	-9.4	-7.5
5	-8.4	-14.7	-7.8	-7.4	-9.2	-8.8
6	-6.0	-8.0	-5.4	-4.1	-5.9	-5.3

^a Grimme's D3 dispersion correction was included and experimental hydration energies of H₂O and H₂PO₄⁻ were employed in all calculations.

^b CPCM/PBE0/6-31+G(d) optimized geometries are used.

Table S4. Average bond distances and standard deviations (Å)

bond label ^a	bond distance	standard deviation
FeL ₁	2.339	0.144
FeL ₂	2.228	0.109
FeL ₃	2.131	0.097
FeL ₄	2.212	0.130
FeL ₅	2.031	0.069
FeL ₆	2.071	0.087
HB ₁	2.166	0.518
HB ₂	1.883	0.168
HB ₃	3.101	0.396
HB ₄	1.783	0.184
HB ₅	1.830	0.199
HB ₆	1.799	0.142
HB ₇	1.701	0.085
HB ₈	1.735	0.145
HB ₉	1.982	0.183

^a See Figure 1 for bond label

Table S5. Calculated $\langle S^2 \rangle$ values.

	spin state	calculated $\langle S^2 \rangle$	exact $\langle S^2 \rangle$
$[\text{Fe}^{\text{II}}(\text{H}_2\text{O})_6]^{2+}$	quintet	6.0046	6.0000
$[\text{Fe}^{\text{II}}(\text{H}_2\text{PO}_4)(\text{H}_2\text{O})_5]^+$	quintet	6.0048	6.0000
$[\text{Fe}^{\text{II}}(\text{H}_2\text{PO}_4)_2(\text{H}_2\text{O})_4]$	quintet	6.0051	6.0000
$[\text{Fe}^{\text{II}}(\text{H}_2\text{PO}_4)_3(\text{H}_2\text{O})_3]^-$	quintet	6.0050	6.0000
$[\text{Fe}^{\text{II}}(\text{H}_2\text{PO}_4)_4(\text{H}_2\text{O})_2]^{2-}$	quintet	6.0050	6.0000
$[\text{Fe}^{\text{II}}(\text{H}_2\text{PO}_4)_5(\text{H}_2\text{O})]^{3-}$	quintet	6.0051	6.0000
$[\text{Fe}^{\text{II}}(\text{H}_2\text{PO}_4)_6]^{4-}$	quintet	6.0051	6.0000
RC	quintet	6.0059	6.0000
INT1_{OH/•OH}	quintet	6.9681	6.0000
INT2_{OH/•OH}	quintet	7.0081	6.0000
INT_{FeIII+•OH}	quintet	7.0080	6.0000
INT_{oxo}	quintet	6.1180	6.0000
$[\text{Fe}^{\text{III}}(\text{H}_2\text{O})_6]^{3+}$	sextet	8.7546	8.7500
$[\text{Fe}^{\text{III}}(\text{H}_2\text{PO}_4)(\text{H}_2\text{O})_5]^{2+}$	sextet	8.7554	8.7500
$[\text{Fe}^{\text{III}}(\text{H}_2\text{PO}_4)_2(\text{H}_2\text{O})_4]^+$	sextet	8.7556	8.7500
$[\text{Fe}^{\text{III}}(\text{H}_2\text{PO}_4)_3(\text{H}_2\text{O})_3]$	sextet	8.7556	8.7500
$[\text{Fe}^{\text{III}}(\text{H}_2\text{PO}_4)_4(\text{H}_2\text{O})_2]^-$	sextet	8.7560	8.7500
$[\text{Fe}^{\text{III}}(\text{H}_2\text{PO}_4)_5(\text{H}_2\text{O})]^{2-}$	sextet	8.7559	8.7500
$[\text{Fe}^{\text{III}}(\text{H}_2\text{PO}_4)(\text{OH})(\text{H}_2\text{O})_4]^+$	sextet	8.7568	8.7500
$[\text{Fe}^{\text{III}}(\text{H}_2\text{PO}_4)_2(\text{OH})(\text{H}_2\text{O})_3]$	sextet	8.7562	8.7500
$[\text{Fe}^{\text{III}}(\text{H}_2\text{PO}_4)_3(\text{OH})(\text{H}_2\text{O})_2]^-$	sextet	8.7557	8.7500
$[\text{Fe}^{\text{III}}(\text{H}_2\text{PO}_4)_4(\text{OH})(\text{H}_2\text{O})]^{2-}$	sextet	8.7560	8.7500
$[\text{Fe}^{\text{III}}(\text{H}_2\text{PO}_4)_5(\text{OH})]^{3-}$	sextet	8.7558	8.7500
$[\text{Fe}^{\text{III}}(\text{HPO}_4)(\text{H}_2\text{O})_5]^+$	sextet	8.7571	8.7500
$[\text{Fe}^{\text{III}}(\text{H}_2\text{PO}_4)(\text{HPO}_4)(\text{H}_2\text{O})_4]$	sextet	8.7561	8.7500
$[\text{Fe}^{\text{III}}(\text{H}_2\text{PO}_4)_2(\text{HPO}_4)(\text{H}_2\text{O})_3]^-$	sextet	8.7558	8.7500
$[\text{Fe}^{\text{III}}(\text{H}_2\text{PO}_4)_3(\text{HPO}_4)(\text{H}_2\text{O})_2]^{2-}$	sextet	8.7560	8.7500
$[\text{Fe}^{\text{III}}(\text{H}_2\text{PO}_4)_4(\text{HPO}_4)(\text{H}_2\text{O})]^{3-}$	sextet	8.7556	8.7500

Spin contamination for every intermediate was examined. It was found that for most intermediates spin contamination problem is negligible, except for **INT1_{OH/•OH}**, **INT2_{OH/•OH}**, and **INT_{FeIII+•OH}**, which exhibit a moderate spin contamination. For the three cases, the •OH is distant from the Fe(III) center and, thus, the spin coupling between •OH and five spins on Fe(III) is very weak. As a consequence, the anti-ferromagnetic coupling (quintet state) and ferromagnetic coupling (sextet state) of these intermediates are very close in energy, resulting in spin-state mixing.⁵³

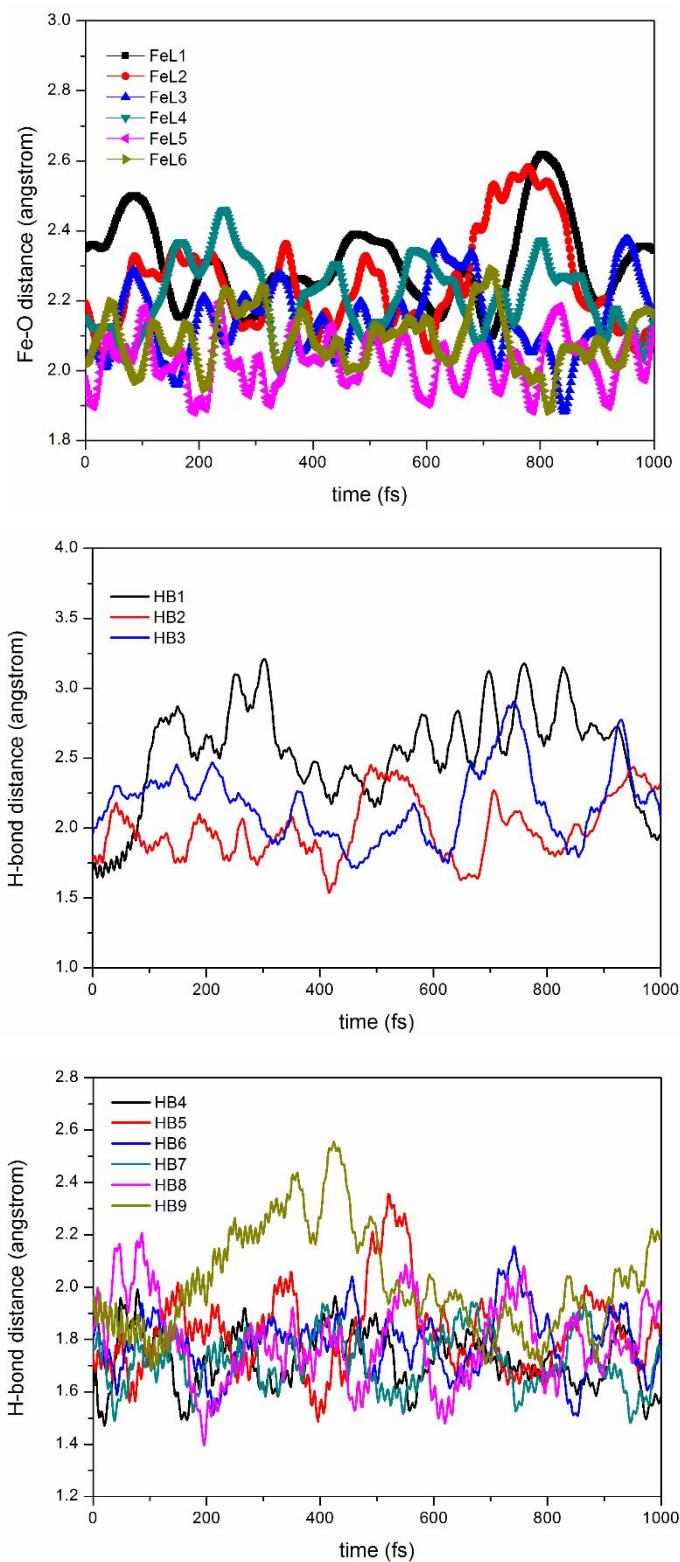


Figure S1. Time evolution of Fe-ligand and H-bond distances for trajectory 2. See Figure 1 for bond label.

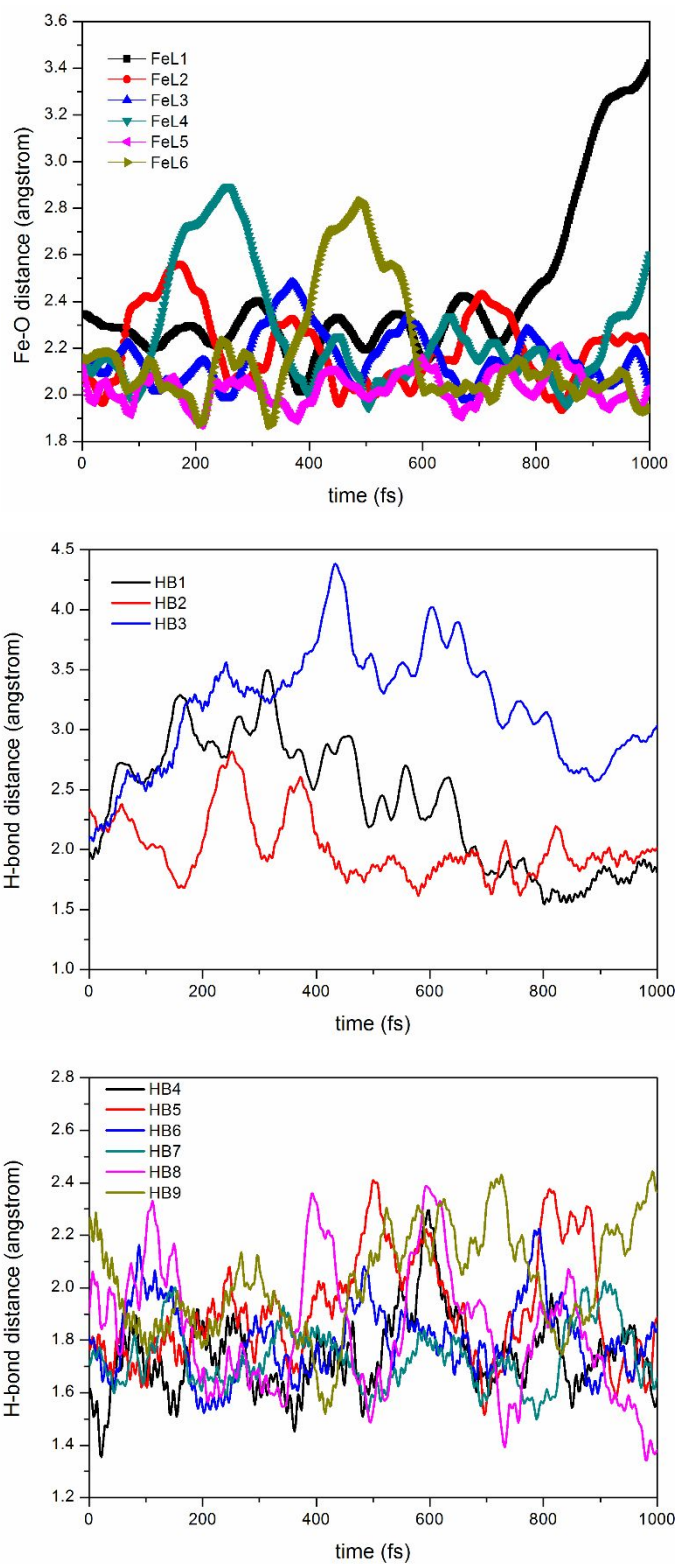


Figure S2. Time evolution of Fe-ligand and H-bond distances for trajectory 3. See Figure 1 for bond label.